ADVANCED ELECTRONIC MATERIALS
www.advelectronicmat.de



# Organic Biomimicking Memristor for Information Storage and Processing Applications

*Gang Liu, Cheng Wang, Wenbin Zhang, Liang Pan, Chaochao Zhang, Xi Yang, Fei Fan, Yu Chen,* and Run-Wei Li**

## 1. Introduction

Developing artificial intelligence that can think, judge, and make decisions like human beings has been a long-dreaming goal of the world.[1–3] In year 2008, HP researchers reported the invention of titanium oxide-based memristor,[4–6] not only for the first time physically implementing the fourth passive circuit component that has been theoretically predicted for ≈40 years but never practically realized[7,8] but also demonstrating that by using the physical property evolution of oxide and chalcogenide materials to fine-tune the resistance response of the devices, emulation of the physiological functions of biological synapses and construction of neuromorphic computers can be made possible.[9–16] To date, tremendous amount of efforts have been devoted to developing biomimicking memristors, most of which have been focused on inorganic materials and devices that require elaborated fabrication procedures.[17] Theoretically speaking, the change of intrinsic properties in organic systems can also be employed to modulate the resistance states and to construct artificial synapses.[18] For instance, both charge transfer and electrochemical redox effects have been used in polymer thin films to consecutively change the device resistances.[19–23] In comparison to the inorganic counterparts, the organic species distinguish themselves with low-cost and easy-fabrication process, mechanical flexibility and deformability, and more importantly, tunable electronic properties via molecular design strategy.[24–30]

Here, we report the first demonstration of memristive behavior of an ethyl viologen diperchlorate [EV($ClO_4$)]/triphenylamine-containing polymer (BTPA-F) organic redox system (**Figure 1**a). The conjugated copolymer of BTPA-F with a closed ring and steric crowded triphenylamine (TPA) group was used in the present study for its rich electrochemical redox behavior,[31,32] while the ethyl viologen diperchlorate (EV($ClO_4$)$_2$) acted as the counter-electrode material for BTPA-F oxidation and a source of the mobile perchlorate ions to stabilize the charged form of the polymer.[20,33–35] Sandwiched between two metal electrodes, the EV($ClO_4$)$_2$/BTPA-F bilayer structure exhibits history-dependent memristive behaviors, which meet the fundamental requirements for mimicking the potentiation and depression processes of a biological synapse. Consequently, a series of synaptic behaviors, including the spike-rate-dependent and spike-timing-dependent plasticity (SRDP and STDP) characteristics, the transition from short-term memory (STM) to long-term memory (LTM), as well as the "learning–forgetting–relearning" process, are successfully emulated in the present organic redox system. These demonstrations show the possibility of using organic materials for the construction of neuromorphic information storage and processing systems.

## 2. Results and Discussion

Prepared via Suzuki coupling polymerization reaction (see Scheme S1 and the Supporting Information for details), the successful synthesis of the conjugated copolymer of BTPA-F was verified through $^1$H NMR, UV–vis absorption spectroscopy and electrochemistry analyses (Figures S1–S3, Supporting Information). When sandwiched between metal electrodes, the 450 nm EV($ClO_4$)$_2$/90 nm BTPA-F bilayer structure (Figure 1b and Figure S4, Supporting Information) exhibits a distinctive history-dependent asymmetric resistive switching behavior at room temperature, as plotted in the current–voltage (*I*–*V*) characteristics of Figure 1c. Initially, the Ta/EV($ClO_4$)$_2$/BTPA-F/Pt memristor shows a small conductivity of ≈ 0.03 S m$^{-1}$ (read at 0.2 V). Upon being subjected to four consecutive positive voltage sweeps of 0 V → 1 V → 0 V, the device conductivity increases incrementally to 0.09 S m$^{-1}$. Afterward, five consecutive negative voltage sweeps of 0 V → –1 V → 0 V have been applied onto the bilayer structure, while the device conductivity decreases continuously from 0.25 to 0.13 S m$^{-1}$ (read at –0.2 V). The small rectifying effect may be ascribed to the difference in the molecular orbital energy levels of the BTPA-F polymer and the EV($ClO_4$)$_2$ counter-electrode material, which in turn influences the charge transport across the EV($ClO_4$)$_2$/BTPA-F junction under electric fields of different polarities. Nevertheless, such a rectifying effect is useful for the single-direction

Dr. G. Liu, W. Zhang, L. Pan, C. Zhang, X. Yang, Prof. R.-W. Li
Key Laboratory of Magnetic Materials and Devices
Ningbo Institute of Materials Technology and Engineering
Chinese Academy of Sciences
Ningbo 315201, P. R. China
E-mail: runweili@nimte.ac.cn
Dr. G. Liu, W. Zhang, L. Pan, C. Zhang, X. Yang, Prof. R.-W. Li
Zhejiang Province Key Laboratory of Magnetic Materials and Application Technology
Ningbo Institute of Materials Technology and Engineering
Chinese Academy of Sciences
Ningbo 315201, P. R. China
C. Wang, F. Fan, Prof. Y. Chen
Institute of Applied Chemistry
East China University of Science and Technology
Shanghai 200237, China
E-mail: chentangyu@yahoo.com

DOI: 10.1002/aelm.201500298

  

ADVANCED ELECTRONIC MATERIALS
www.advelectronicmat.de

www.MaterialsViews.com

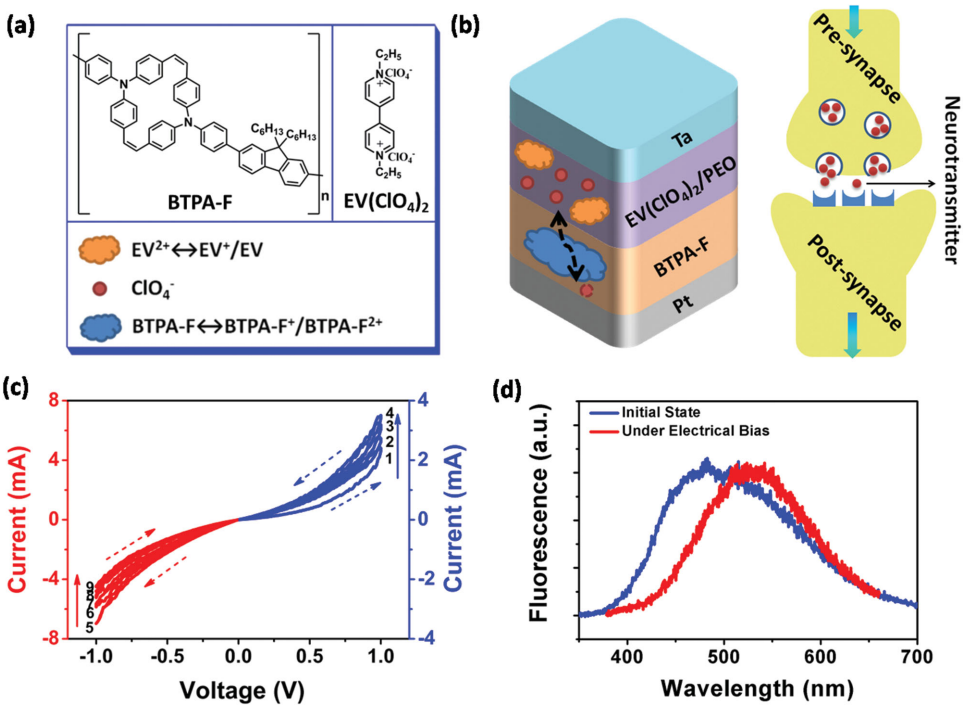


**Figure 1.** a) Chemical structures of BTPA-F and $EV(ClO_4)_2$ as well as the electrochemical redox reaction of the $EV(ClO_4)_2$/BTPA-F bilayer structure. b) Schematic illustration of the Ta/$EV(ClO_4)_2$/BTPA-F/Pt memristor and the biological synapse. c) The current–voltage characteristics of the Ta/$EV(ClO_4)_2$/BTPA-F/Pt memristor showing nonlinear transmission behavior similar to that of a biological synapse. d) The fluorescence of the $EV(ClO_4)_2$/BTPA-F bilayer structure in the initial state and under electrical bias.

transmission of information in biological synapses.[36,37] Being different from the bistable resistive switching showing abrupt resistance or conductance jumps for memory applications,[38–40] the electrical transition observed herein demonstrates a smoother tuning of the device conductance during the voltage sweeping processes, and the *I–V* loop of each subsequent sweep picks up where the last sweep left off or partially overlaps with each other. Together with a "pinch-off" feature in the *I–V* curves, this resistive switching phenomenon is definitely the characteristic of a memristor device.[41] A better illustration of the continuous modulation of the device conductance, demonstrated as the sweeping voltage and responding current versus time characteristics, are shown in Figure S5 (Supporting Information). Therefore, defined as the synaptic weight of a biomimicking memristor, the conductance of the $EV(ClO_4)_2$/BTPA-F device can be memorized and modulated continuously by consecutive voltage stimulations, which is in close similarity to the nonlinear transmission characteristics of biological synapses.

As shown in Figure 1a, the conjugated copolymer of BTPA-F carries a closed ring and steric crowded TPA group. The applied positive electric field can remove the unshared pair of electrons from the nitrogen atom of the TPA moiety, oxidize the polymer and introduce impurity energy levels into the band gap of the material.[31,32,42] As such, the conductance of the BTPA-F polymer and the device can be significantly enhanced via intra- and interchain hopping through these charged centers. In the meanwhile, the cations of the 4,4′-bipyridine salt is reduced as the counter electrode materials.[20] The perchlorate anions are then driven by the external electric field to drift toward and to neutralize the positively charged nitrogen atoms of the BTPA moiety, making the entire redox system electrically neutral and stable.[33–35] Under the reversed biased electric field, the reduction of the BTPA moieties, oxidation of the 4,4′-bipyridine species and the back transfer of the perchlorate anions switch the device back to its initial low conductance state. Fluorescence spectroscopic measurement has also been conducted in situ to verify the proposed electrochemical redox mechanism. To record the optical signals, the top tantalum electrode was replaced with indium-tin oxide electrode that is almost transparent to both the excitation beam of 325 nm wavelength and the emission beam in the visible region. As shown in Figure 1d, the pristine $EV(ClO_4)_2$/BTPA-F bilayer structure shows a broad emission band over the wavelength range of 400–650 nm, with the emission maximum centered at ≈480 nm. The fluorescence can be attributed to the presence of the dimeric and closed ring structure of the two triphenylamine groups.[42–45] When the device is subjected to electrical bias of a few volt, significant redshift (≈45 nm) of the emission maximum can be observed. The change in the lineshape of the fluorescence spectrum of the polymer under electrical bias indicates the occurrence of the two-step oxidation of the dimeric triphenylamine group, which is in good agreement with the reported phenomena[43] and thus confirms that the memristive switching of the device is accompanied by electrochemical redox reaction of the $EV(ClO_4)_2$/BTPA-F bilayer structure. With the device structure being similar to that of an electrochromic device, the UV–vis absorption spectra of the $EV(ClO_4)_2$/BTPA-F bilayer also demonstrate gradually enhanced absorbance when being subjected to applied voltages (Figure S6, Supporting Information). Samples with larger active area also exhibits visible color changes under the

electrical biases, again confirming electrochemical redox mechanism of the present devices.

The potentiation and depression of a biological synapse, which are considered as the neurobiological basis of the human brain memory functions,[46] are usually achieved through action potential spikes. Spontaneous relaxation of the synaptic connection also exists simultaneously to compete with the potentiation process upon the application of stimuli. As shown in **Figure 2**a, four consecutive voltage pulse stimuli with the amplitude of 1 V, duration of 10 ms, and period of 2 s have been used to exam the synaptic weight response of the $EV(ClO_4)_2$/BTPA-F memristor, while a low read voltage of 0.2 V was used to avoid significant disturbance on device conductance. Upon the application of each voltage pulse, the device conductance first increases abruptly, followed by a rapid decay to a lower level. Though the time interval between the stimulation is relatively longer as compared to those reported in the literature,[11] a net increase of the device conductance, which equals the fundamental activity of plasticity of biological synapses, is still observed. The origin of the synaptic relaxation is probably arising from the spontaneous back diffusion of the perchlorate counter ions under the concentration gradient field.[11,12] The overall increase of the device conductance is further enhanced with the increasing number of voltage pulse stimulations, which well resembles the paired-pulse facilitation (PPF) and posttetanic potentiation (PTP) behaviors in biological systems.[47,48]

On the other hand, the current response spikes and rapid decay processes are also observed when negative voltage pulses with the amplitude of −1 V, duration of 10 ms, and period of 2 s are applied onto the $EV(ClO_4)_2$/BTPA-F memristor, despite for the overall decrease of the device conductance with the number of voltage pulse stimulations, which may be due to the reverse redox reaction under electric field with opposite polarity (Figure 2b). Figure 2c shows the current response of the $EV(ClO_4)_2$/BTPA-F memristor upon being subjected to 50 consecutive positive voltage pulses and immediately 50 following consecutive negative voltage pulses. Obviously, the synaptic weight of the $EV(ClO_4)_2$/BTPA-F memristor has been potentiated or depressed with the consecutive positive or negative stimuli, respectively. In accordance with the back-diffusion-induced relaxation process, a gap between the current monitored at the end of the potentiation process and that monitored at the beginning of the depression process exists.

The potentiation of the synaptic weight can also be achieved by increasing the frequencies of the applied voltage pulses, thus emulating the SRDP of biological synapses.[49,50] By fixing the numbers of the voltage pulse stimulations applied onto the $EV(ClO_4)_2$/BTPA-F memristor at a constant of 10 while changing the frequency from 1 to 20 Hz (or equivalently, changing the pulse-to-pulse intervals from 1 to 0.05 s), it is found that the more frequently the synapse is being stimulated, the higher the currents become (**Figure 3**a). In order to

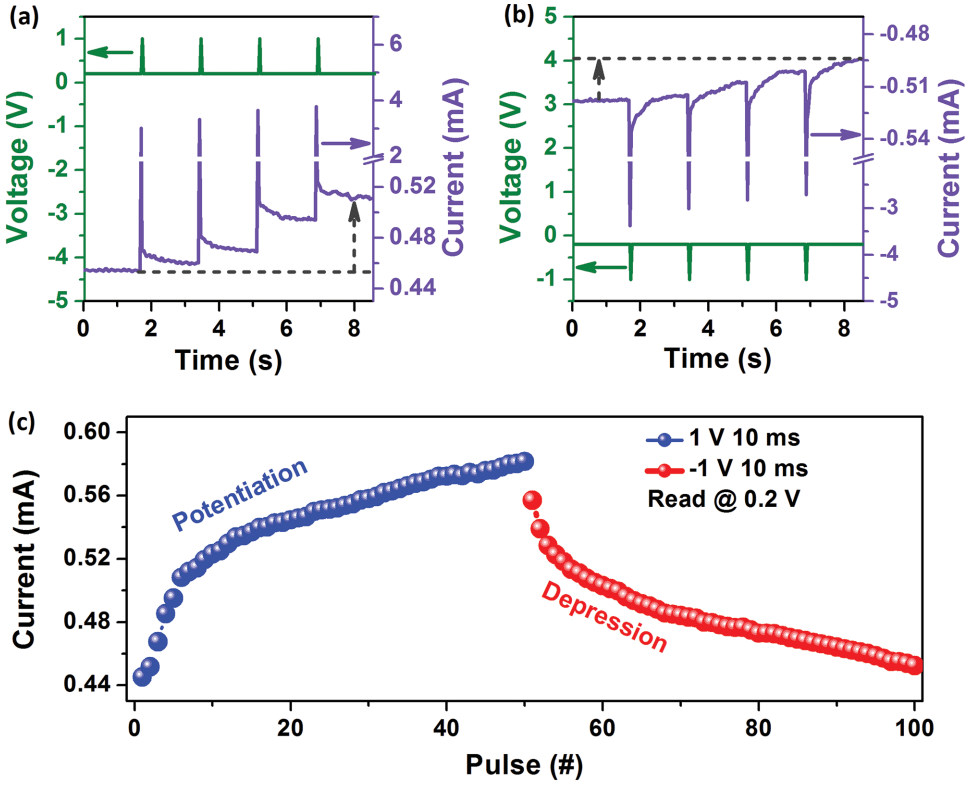


**Figure 2.** Potentiation and depression processes of the $EV(ClO_4)_2$/BTPA-F memristor. The voltage– and current–time characteristics recorded under the a) positive and b) negative voltage pulse stimulations showing spike response, spontaneous decay, and overall enhancement or weakening of the device conductance. c) The current in response to a series of positive and negative voltage stimulations showing the respective potentiation and depression of the device synaptic connection. The amplitude, duration, and period of the voltage pulses are ±1 V, 10 ms, and 2 s, respectively. The current responses are monitored with a small voltage of ±0.2 V.

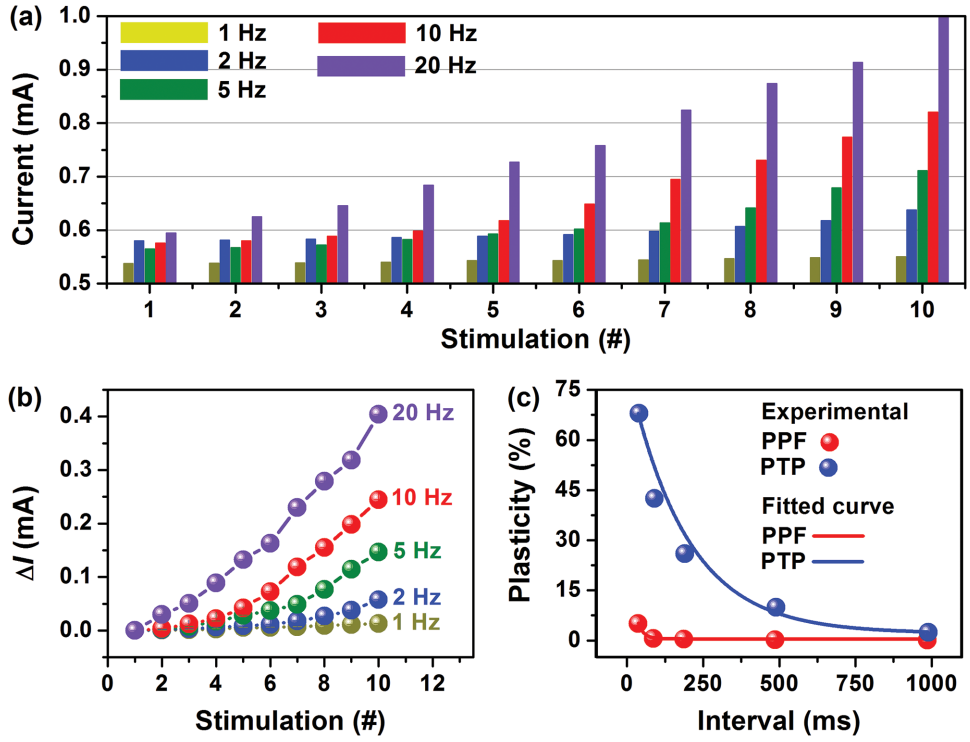


**Figure 3.** Frequency-dependent synaptic potentiation and SRDP of the $EV(ClO_4)_2$/BTPA-F memristor. Evolution of the device a) current and b) current change ($\Delta I$) with ten voltage pulse stimulations at different frequencies. c) Plasticity versus pulse interval characteristics of the device. The fitting of PPF and PTP are according to the equation of $y = y_0 + A_{exp}(-x/t)$. The amplitude and duration of the voltage pulses are 1 V and 10 ms, respectively. The current responses are monitored with a small voltage of 0.2 V.

quantitatively analyze the increment of the current recorded at each frequency, the relative changes of currents versus stimulating numbers were replotted in Figure 3b. At the frequency of 1 Hz, there is no obvious increase of the device current with the stimulation numbers. When the frequency reaches 20 Hz, the device current has been increased by more than 30-fold. This suggests that the present device acts as a high-pass filter. Furthermore, the plasticity of the memristor device can be estimated according to the PPF and PTP models with the following equations (Figure 3c)[47]

$$\mathrm{PPF} = (I_2 - I_1)/I_1 \times 100\% \quad (1)$$

$$\mathrm{PTP} = (I_{10} - I_1)/I_1 \times 100\% \quad (2)$$

where $I_1$, $I_2$, and $I_{10}$ are the currents recorded after the first, second, and tenth voltage pulse stimulations, respectively. An exponential dependence of the device plasticity on the pulse-to-pulse time interval can be clearly observed.

Taking the Pt and Ta electrodes as the presynaptic and postsynaptic neurons, respectively, such a frequency-dependent potentiation of the synaptic weight would be attributed to the spatial and temporal interaction between the voltage pulse stimulus (or spike) and the ionic excitatory postsynaptic current (EPSC). As shown in **Figure 4**a, a single presynaptic spike with the amplitude of 1.5 V and the duration of 10 ms can trigger an EPSC that can last for ≈100 ms. Due to the inertia of the ionic flux, the life time of the EPSC is much longer than that of the triggering spike. Thus, if multiple stimulations with the pulse-to-pulse time intervals comparable to or shorter than the life time of the EPSC have been applied onto the $EV(ClO_4)_2$/BTPA-F memristor, the overlap between the voltage pulse stimulation and the EPSC will of course accelerate the ionic flux and thus produce a more effective potentiation of the synaptic weight. Nevertheless, spatial and temporal interaction also exists between the pre- and postsynaptic stimulations through EPSC or inhibitory postsynaptic current to modulate the synaptic connection synergistically.[51] For the purpose of demonstration, a pair of voltage pulses, both of which consist of a positive and a negative pulses with the amplitude, duration, and separation are ±1.5 V, 10 ms, and 2 s, respectively, have been applied onto the Pt and Ta electrodes as the pre- and postsynaptic spikes. The profiles of the presynaptic and postsynaptic spikes are shown in Figure 4b. Similar to that defined by Equation (3), change of the synaptic weight ($\Delta W$) can be calculated as $(I_2 - I_1)/I_1$, where $I_1$ and $I_2$ are the currents recorded before and 10 min after the spike-pair application, respectively. $\Delta t$ is defined as the time interval between the presynaptic and postsynaptic spikes ($\Delta t = t_{pre} - t_{post}$). When the presynaptic spike arrives before the postsynaptic spike (with $\Delta t < 0$), the synaptic weight becomes depressed; when the postsynaptic spike arrives earlier that the presynaptic spike (with $\Delta t > 0$), the synaptic weight gets potentiated (Figure 4c). In addition, both the potentiation and depression of the synaptic weights show negative dependence on the time interval between the spike pairs, where a smaller $\Delta t$ produces a more heavily potentiated or depressed

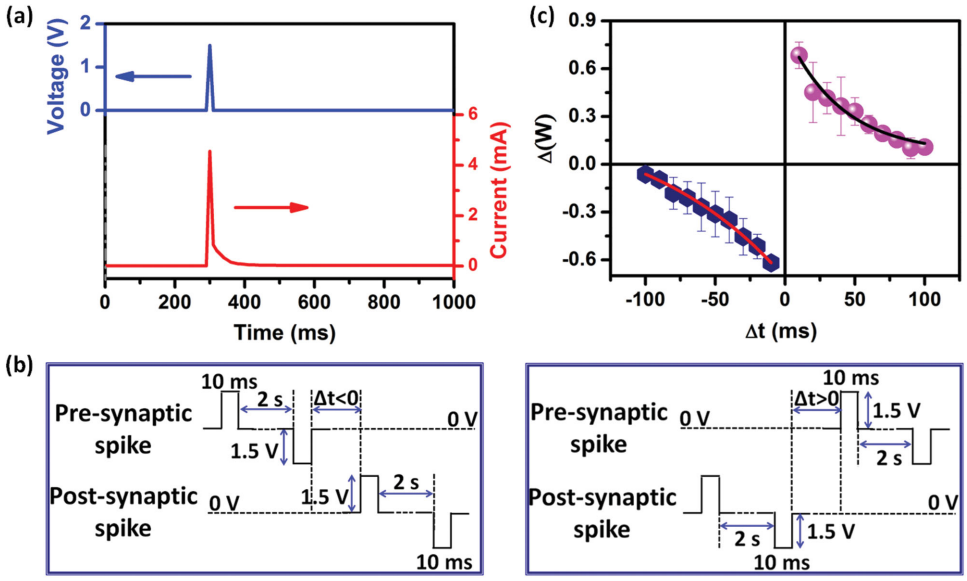


**Figure 4.** Spike-timing-dependent plasticity of the BTPA-F/EV$(ClO_4)_2$ memristor. a) Evolution of an excitatory postsynaptic current stimulated with the voltage pulse stimulation with the amplitude and duration of 1.5 V and 10 ms, respectively. b) The profiles of the presynaptic and postsynaptic spikes consisting of a voltage pulse pair with the amplitude, duration, and separation of ±1.5 V, 10 ms, and 2 s, respectively. c) Change of the synaptic weight with the relative timing $\Delta t$ of the presynaptic and postpresynaptic spike-pair application.

synaptic weight accordingly. Thus, through the precise control of the timing between the spike-pair applications, a STDP of the biological synapses has been successfully emulated.[52,53]

In human brains, the memory is by no means eternal. The transient or STM, which only lasts for seconds or minutes, could be easily interrupted by accidental electrical shock or decay rapidly with time.[47,54,55] In obvious contrast, the LTM, involving permanent changes in certain synaptic structures, can be sustained for hours, days, weeks, months, or years.[56] Thus, understanding the mysteries of the activity-dependent changes in the synaptic connections will be helpful for enhancing the memory capability.[57,58] Strategically, transition from STM to LTM can be achieved through consolidation with repeated stimulations (or rehearsal) in the present EV$(ClO_4)_2$/BTPA-F memristors (**Figure 5**a).[59,60] For instance, identical voltage pulse stimulations with fixed amplitude, duration, and period but different numbers show strong influence on the memory retention or loss performance of the device (Figure 5b). After a fast decay in the initial stage, the synaptic weight of the device, which is the normalized current value obtained with the stimulating voltage pulses of 1 V/10 ms and reading voltage pulse of 0.2 V/10 ms, respectively, gradually approaches to an intermediate level. This indicates the coexistence of STM and LTM in the EV$(ClO_4)_2$/BTPA-F memristor. It is noteworthy that upon being stimulated for only ten times, the synaptic connection gets almost vanished after 15 s. When the number of voltage pulse stimulations is increased from 10 to 60, an obvious decrease in the memory loss speed and simultaneous increase in the remaining memory can be established. Nevertheless, LTM still fades with time, suggesting that the synaptic connections relax with time, but with a much lower speed than that of the STM.[11] A more accurate time constant of the memory decay process, as well as the stabilized synaptic weight, can be obtained by fitting the retention curve with the modified Kohlrausch equation that is widely used in psychology and popular in the recent research of biomimicking memristors[61–63]

$$I(t) = I_0 + A\exp(-t/\tau) \quad (3)$$

where $I(t)$ and $I_0$ are the synaptic weights retained at the time of $t$ and at the stabilized state, respectively, A is the preexponential factor and $\tau$ is relaxation time constant which can be used to evaluate the forgetting speed of the memristor. As shown in Figure 5c, both the stable synaptic weight and the relaxation constant $\tau$ get significantly reinforced with increase in the stimulating number, making the transition from STM to LTM possible in the present EV$(ClO_4)_2$/BTPA-F memristor.

The "learning–forgetting–relearning" process, which usually involves the "learning–experience" behavior of human beings,[12,64] has also been achieved in the present study. After being stimulated by 40 consecutive voltage pulses (Figure 5d) and then decayed spontaneously for 5 min to an intermediate state (Figure 5e), the synaptic weight of the EV$(ClO_4)_2$/BTPA-F memristor only takes nine stimulations to be recovered to its end level of the first learning stage (Figure 5f). The relearning of the previously memorized information can strengthen the memory capability significantly, as the following relaxation of the synaptic weight reaches a much higher level with a much slower speed (Figure 5g). Afterward, four stimuli are adequate to restore the memory level again (Figure 5h). This indicates that the relearning of the blurry information can be easier upon reexercises,[65,66] and a behavior similar to the STM-to-LTM transition occurs. Again, the occurrence of redox reaction inside the EV$(ClO_4)_2$/BTPA-F bilayer structure accounts for the observed "learning–forgetting–learning" behavior. As the redox reaction and the migration of perchlorate counterions continues, the amount of charged nitrogen species and energy band diagram of the system get modulated consecutively, leading to the

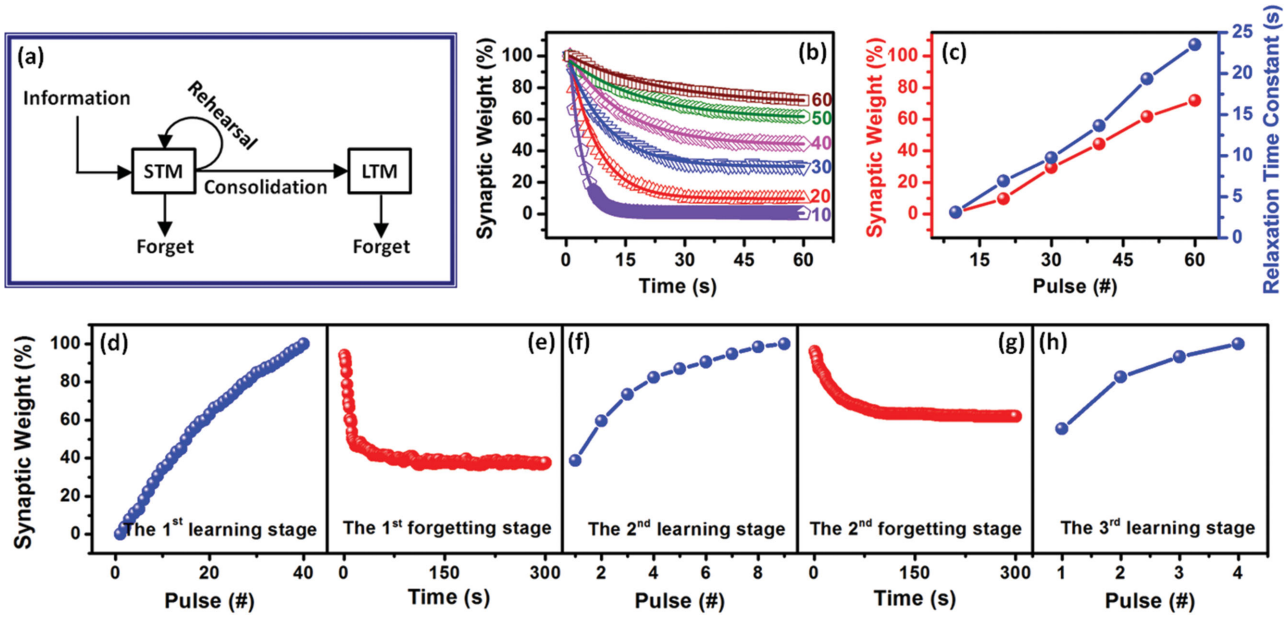


**Figure 5.** Memory enhancement of the $EV(ClO_4)_2$/BTPA-F memristor. a) Schematic illustration of the STM to LTM transition. b) Experimental (symbols) and fitted (solid lines) memory retention performance after being subjected to different numbers of identical voltage pulse stimulations. c) Evolution of the relaxation time constant ($\tau$) and the stabilized synaptic weight ($I_o$) along with the stimulating numbers. d–h) Demonstration of the "learning–forgetting–relearning" process. The amplitude, duration, and period of the voltage pulses are 1 V, 10 ms, and 2 s, respectively. The current responses are monitored with a small voltage of 0.2 V.

gradual modulation (enhancement) of the conductance of the $EV(ClO_4)_2$/BTPA-F bilayer structure. When the external electric field is removed, the reverse redox of the $EV(ClO_4)_2$/BTPA-F pair, wherein the charged BTPA moieties are reduced while the 4,4′-bipyridine species are reoxidized, occurs spontaneously and proceeds with time to minimize the total energy level of the system. Consequently, the conductance or the synaptic weight of the memristive device relaxes. It is noteworthy that the redox behavior of the $EV(ClO_4)_2$/BTPA-F system and migration of perchlorate anions will result in certain degree of permanent changes of the organic layers, in terms of the oxidative state and/or the microscopic changes in the structure or morphologies. As a result, the synaptic weight does not relax to the initial level before learning. When thicker films of the bilayer system are used, the spontaneous reverse redox behavior of the $EV(ClO_4)_2$/BTPA-F pair and the back diffusion of the perchlorate anions can be suppressed, leading to a slower "forgetting" process and higher level of the remained memory. Nevertheless, as the organic system "remembers" the redox processes it undergoes, fewer amount of further stimulus can set it to the previously set state.

## 3. Conclusion

To summarize, based on the intrinsic reversible redox behaviors of a viologen/triphenylamine-polymer bilayer, organic memristor with the simple structure of Ta/$EV(ClO_4)_2$/BTPA-F/Pt and history-dependent resistive switching behaviors was constructed. Essential synaptic functions, including the nonlinear single-direction transmission, potentiation, and depression of the synaptic connection, SRDP, STDP, STM-to-LTM transition, as well as the training process that resembles the learning/memory functions of biological systems, have been demonstrated. With the synaptic plasticity behaviors achieved in the present device satisfying the basic requirements for neuromorphic computing, more efforts should be devoted in the future to the designing and construction of deformatively interconnected networks of biomimicking synapses for large-scale neuromorphic circuits.

## 4. Experimental Section

*Synthesis of Monomers and Polymer:* *N,N′*-Diphenyl-4-bromoaniline dimer (BTPA) was synthesized according to ref. [30] and [31] (Scheme S1, Supporting Information). The BTPA-F conjugated copolymer was synthesized via Suzuki coupling polymerization of BTPA with 2,2′-(9,9-dihexyl-9H-fluorene-2,7-diyl)bis (4,4,5,5-tetramethyl-1,3,2-dioxaborolane) (denoted as chemical 1 for short). To be specific, a mixture of BTPA (230 mg, 0.33 mmol) and **1** (230 mg, 0.40 mmol) was dissolved in a 9 mL mixed solution of toluene and water ($v/v = 2/1$) in a 25 mL Schlenk tube. After degassing with nitrogen for 15 min, 3 mg of $Pd(PPh_3)_4$ was introduced into the flask. Then the reaction mixture was degassed for another 15 min, followed by being stirred at 100 °C for 36 h. Afterward, the green mixture was allowed to cool down to room temperature, poured slowly into 100 mL methanol, filtered with Buchner funnel and redissolved in $CHCl_3$. The obtained chloroform solution was passed through a column of siliceous earth quickly to remove the metal catalyst. After evaporating the excess solvent, the crude polymer product was subjected to Soxhlet extraction sequentially with acetone and hexane to remove the unreacted monomers. The obtained solid was then redissolved in $CHCl_3$ and poured into methanol to give the green polymer with a yield of 45.5% (132 mg). $^1$H NMR (400 MHz, $CDCl_3$, ppm): 7.73–7.74 (m, 4H), 7.52 (m, 6H), 7.13–7.14 (m, 4H), 7.00–7.04 (m, 16H), 6.61 (d, 4H), 2.00–2.02 (m, 4H), 1.03–1.09 (m, 16H), 0.77–0.82 (m, 6H). $M_n = 2.24 \times 10^4$, $M_w/M_n = 2.17$.

*Device Fabrication and Characterization*: The memristor behaviors of polymer/viologen system were examined in Ta/EV$(ClO_4)_2$/BTPA-F/Pt structures. The Pt/Ti/$SiO_2$/Si substrates (Hefei Ke Jing Materials technology Co., LTD.) were precleaned in the ethanol, acetone, and isopropanol in an ultrasonic bath, each for 30 min in that order. The BTPA-F solution of 6 mg $mL^{-1}$ was prepared by dissolving the polymer powders in cyclohexanone. The as-prepared solutions were filtrated through polytetrafluoroethylene membrance microfilters with a pore size of 0.45 μm to remove any dissolved particles. The BTPA-F functioning layers were then deposited by spin casting 50 μL solution of the polymer onto the precleaned Pt/Ti/$SiO_2$/Si substrate at a spinning speed of 600 rpm for 15 s and then at 1000 rpm for 50 s, followed by being vacuum dried at 50 °C overnight. The electrolyte solution was prepared according to the reported method.[16] The Ta electrodes of 60 nm thickness were deposited by E-beam evaporation through a metal shadow mask at room temperature under reduced pressure ($10^{-5}$ Pa). The electrical properties of the Ta/EV$(ClO_4)_2$/BTPA-F/Pt devices were measured with a Keithley 4200 semiconductor characterization system under s sweep or pulse mode at room temperature.

## Supporting Information

Supporting Information is available from the Wiley Online Library or from the author.

## Acknowledgements

G.L., C.W., and W.Z. contributed equally to this work. This work was supported by the State Key Project of Fundamental Research of China (973 Program, 2012CB933004), National Natural Science Foundation of China (51303194, 11474295, 61328402, 51333002, and 21074034), the Instrument Developing Project of the Chinese Academy of Sciences (YZ20132), the Youth Innovation Promotion Association of the Chinese Academy of Sciences, Ningbo Natural Science Foundations (2013A610031), and Ningbo International Cooperation Projects (2012D10018 and 2014D10005).

Received: September 9, 2015
Revised: September 23, 2015
Published online:

[1] J. Von Neumann, *The Computer and the Brain*, 2nd ed., Yale University Press, New Haven, CT **2000**, p. 327.
[2] G. Perea, M. Nevarrete, A. Araque, *Trends Neurosci.* **2009**, *32*, 421.
[3] G. Perea, A. Araque, *J. Neurosci.* **2005**, *25*, 2192.
[4] D. B. Strukov, G. S. Snider, D. R. Stewart, R. S. Williams, *Nature* **2008**, *453*, 80.
[5] G. S. Snider, *IEEE/ACM Int. Symp. Nanoscale Archit.*, Anaheim, CA, June **2008**, p. 85.
[6] J. J. Yang, D. B. Strukov, D. R. Stewart, *Nat. Nanotechnol.* **2013**, *8*, 13.
[7] L. O. Chua, *IEEE Trans. Circuit Theory* **1971**, *CT18*, 507.
[8] L. O. Chua, S. M. Kang, *Proc. IEEE* **1976**, *64*, 209.
[9] S. H. Jo, T. Chang, I. Ebong, B. B. Bhadviya, P. Mazumder, W. Lu, *Nano Lett.* **2010**, *10*, 1297.
[10] T. Ohno, T. Hasegawa, T. Tsuruoka, K. Terabe, J. K. Gimzewski, M. Aono, *Nat. Mater.* **2011**, *10*, 591.
[11] T. Chang, S. H. Jo, W. Lu, *ACS Nano* **2011**, *5*, 7669.
[12] Z. Q. Wang, H. Y. Xu, X. H. Li, H. Yu, Y. C. Liu, X. J. Zhu, *Adv. Funct. Mater.* **2012**, *22*, 2759.
[13] P. Krzysteczko, J. Munchenberger, M. Schafers, G. Reiss, A. Thomas, *Adv. Mater.* **2012**, *24*, 762.
[14] D. Kuzum, R. G. D. Jeyasingh, B. Lee, H. S. P. Wong, *Nano Lett.* **2012**, *12*, 2179.
[15] Y. Li, Y. P. Zhong, L. Xu, J. J. Zhang, X. H. Xu, H. J. Sun, X. S. Miao, *Sci. Rep.* **2013**, *3*, 1619.
[16] Y. Li, Y. P. Zhong, J. J. Zhang, L. Xu, Q. Wang, H. J. Sun, H. Tong, X. M. Cheng, X. S. Miao, *Sci. Rep.* **2014**, *4*, 4906.
[17] F. Pan, S. Gao, C. Chen, C. Song, F. Zeng, *Mater. Sci. Eng. Res.* **2014**, *83*, 1.
[18] Y. Chen, G. Liu, C. Wang, W. Zhang, R.-W. Li, L. Wang, *Mater. Horiz.* **2014**, *1*, 489.
[19] A. Bandyopadhyay, S. Sahu, M. Higuchi, *J. Am. Chem. Soc.* **2011**, *133*, 1168.
[20] R. Kumar, R. G. Pillai, N. Pekas, Y. Wu, R. L. McCreery, *J. Am. Chem. Soc.* **2012**, *134*, 14869.
[21] V. Erokhin, T. Berzina, K. Gorshkov, P. Camorani, A. Pucci, L. Ricci, G. Ruggeri, R. Sigala, A. Schüz, *J. Mater. Chem.* **2012**, *22*, 22881.
[22] B. Hu, X. Zhu, X. Chen, L. Pan, S. Peng, Y. Wu, J. Shang, G. Liu, Q. Yan, R.-W. Li, *J. Am. Chem. Soc.* **2012**, *134*, 17408.
[23] C. Wang, G. Liu, Y. Chen, R.-W. Li, W. Zhang, L. Wang, B. Zhang, *J. Mater. Chem. C* **2015**, *3*, 664.
[24] J. C. Scott, L. D. Bozano, *Adv. Mater.* **2007**, *19*, 1452.
[25] Q.-D. Ling, D.-J. Liaw, C. Zhu, D. S.-H. Chan, E.-T. Kang, K.-G. Neoh, *Prog. Polym. Sci.* **2009**, *33*, 917.
[26] B. Cho, S. Song, Y. Ji, T.-W. Kim, T. Lee, *Adv. Funct. Mater.* **2011**, *21*, 2806.
[27] C.-L. Liu, W.-C. Chen, *Polym. Chem.* **2011**, *2*, 2169.
[28] W.-P. Lin, S.-J. Liu, T. Gong, Q. Zhao, W. Huang, *Adv. Mater.* **2014**, *26*, 570.
[29] G. Y. Wen, Z. J. Ren, D. M. Sun, T. J. Zhang, L. L. Liu, S. K. Yan, *Adv. Funct. Mater.* **2014**, *24*, 3446.
[30] D. M. Sun, Z. M. Yang, Z. J. Ren, H. H. Li, M. R. Bryce, D. G. Ma, S. K. Yan, *Chem. Eur. J.* **2014**, *20*, 16233.
[31] a) Y. Shirota, *J. Mater. Chem.* **2000**, *10*, 1; b) Y. Shirota, *J. Mater. Chem.* **2005**, *15*, 75.
[32] Y. Song, C. Di, X. Yang, S. Li, W. Xu, Y. Liu, L. Yang, Z. Shuai, D. Zhang, D. Zhu, *J. Am. Chem. Soc.* **2006**, *128*, 15940.
[33] R. J. Mortimer, A. L. Dyer, J. R. Reynolds, *Displays* **2006**, *27*, 2.
[34] B. Liu, A. Baszczyk, M. Mayor, T. Wandlowski, *ACS Nano* **2011**, *5*, 5662.
[35] B. Han, Z. Li, T. Wandlowski, A. Baszczyk, M. Mayor, *J. Phys. Chem. C* **2007**, *111*, 13855.
[36] M. E. Bear, B. W. Connors, M. A. Paradiso, *Neuroscience: Exploring the Brain*, High Education Press, Beijing **2007**, p. 761.
[37] R. C. Aktinson, R. M. Shiffrin, *The Psychology of Learning and Motivation: Advances in Research and Theory*, Academic Press, New York **1968**, p. 89.
[38] Y.-K. Fang, C.-L. Liu, C. Li, C.-J. Lin, R. Mezzenga, W.-C. Chen, *Adv. Funct. Mater.* **2010**, *20*, 3012.
[39] N.-G. Kang, B. Cho, B.-G. Kang, S. Song, T. Lee, J.-S. Lee, *Adv. Mater.* **2012**, *24*, 385.
[40] S. G. Hahm, N.-G. Kang, W. Kwon, K. Kim, Y.-G. Ko, S. Ahn, B.-G. Kang, T. Chang, J.-S. Lee, M. Ree, *Adv. Mater.* **2012**, *24*, 1062.
[41] L. Chua, *Appl. Phys. A: Mater. Sci. Process.* **2011**, *102*, 765.
[42] Y. Zhao, C. Ye, Y. Qiao, W. Xu, Y. Song, D. Zhu, *Tetrahedron* **2012**, *68*, 1547.
[43] Y. Cui, Q. Chen, D.-D. Zhang, J. Cao, B.-H. Han, *J. Polym. Sci., Part A: Polym. Chem.* **2010**, *48*, 1310.
[44] M. Yang, D. xu, W. Xi, L. Wang, J. Zheng, J. Huang, J. Zhang, H. Zhou, J. Wu, Y. Tian, *J. Org. Chem.* **2013**, *78*, 10344.
[45] C. Quinton, V. Alain-Rizzo, C. Dumas-Verdas, F. Miomandre, G. Clavier, P. Aubedert, *Chem. Eur. J.* **2015**, *21*, 2230.
[46] P. D. Grimwood, S. J. Martin, R. G. M. Morris, *Synapse*, John Hopkins University Press, Baltimore, MD **2001**, p. 519.

  

[47] P. P. Atluri, W. G. Regehr, *J. Neurosci.* **1996**, *16*, 5661.
[48] K. L. Magleby, *J. Physiol.* **1973**, *234*, 327.
[49] S. Li, F. Zeng, C. Chen, H. Liu, G. Tang, S. Gao, C. Song, Y. Lin, F. Pan, D. Guo, *J. Mater. Chem.* **2013**, *1*, 5292.
[50] H. Markram, A. Gupta, A. Uziel, Y. Wang, M. Tsodyks, *Neurobiol. Learn. Mem.* **1998**, *70*, 101.
[51] G. Q. Bi, M. M. Poo, *J. Neurosci.* **1998**, *15*, 10464.
[52] Y. Dan, M.-M. Poo, *Neuron* **2004**, *44*, 23.
[53] N. Caporale, Y. Dan, *Annu. Rev. Neurosci.* **2008**, *31*, 25.
[54] J. A. Kauer, R. C. Malenka, *Nat. Rev. Neurosci.* **2007**, *8*, 844.
[55] G. Daoudal, D. Debanne, *Learn. Mem.* **2003**, *10*, 456.
[56] C. H. Bailey, E. R. Kandel, *Annu. Rev. Physiol.* **1993**, *55*, 397.
[57] M. Makhinson, J. K. Chotiner, J. B. Watson, T. J. O'Dell, *J. Neurosci.* **1999**, *19*, 2500.
[58] G. G. Turrigiano, K. R. Leslie, N. S. Desai, L. C. Rutherford, S. B. Nelson, *Nature* **1998**, *391*, 892.
[59] K. A. Paller, A. D. Wagner, *Trends Cognit. Sci.* **2002**, *6*, 93.
[60] F. I. Craik, M. J. Watkins, *J. Verb. Learning Verb. Behav.* **1973**, *12*, 599.
[61] B. Sturman, E. Podivilov, M. Gorkunov, *Phys. Rev. Lett.* **2003**, *91*, 176602.
[62] J. T. Wixted, E. B. Ebbesen, *Psychol. Sci.* **1991**, *2*, 409.
[63] D. C. Rubin, S. Hintin, A. Wenzel, *J. Exp. Psychol. Learn.* **1999**, *25*, 1161.
[64] W. T. Greennough, J. E. Black, C. S. Wallace, *Child Dev.* **1987**, *58*, 539.
[65] M. Joëls, Z. Pu, O. Wiegert, M. S. Oitzl, H. J. Krugers, *Trends Cognit. Sci.* **2006**, *10*, 152.
[66] O. Jensen, J. E. Lisman, *Learn. Mem.* **1996**, *3*, 279.